

Constraint on solar axions from seismic solar models

Satoru Watanabe*, Hiromoto Shibahashi

Department of Astronomy, School of Science, The University of Tokyo, 7-3-1

Hongo, Bunkyo-ku, Tokyo 113-0033, Japan

Abstract

We reexamine the theoretical limit on the axion coupling to two photons, $g_{a\gamma\gamma}$, in the light of a new solar model (seismic solar model) and the latest solar neutrino observations, the Super-Kamiokande and the Sudbury Neutrino Observatory (SNO). From the comparison of the theoretically expected and the measured neutrino fluxes, we set a limit $g_{a\gamma\gamma} < 4.0 \times 10^{-10} \text{ GeV}^{-1}$. This limit based on a new procedure is about a factor of 3 improvement over the previous theoretical limit and a more severe limit than the solar axion experiments. Therefore this limit is the most stringent limit on solar axions.

Key words: Axion; Helioseismology; Solar neutrino; Solar interior

PACS: 14.80.Mz, 96.60.Ly, 26.65.+t, 96.60.Jw

* Corresponding author.

Email address: watanabe@astron.s.u-tokyo.ac.jp (Satoru Watanabe).

1 Introduction

The axion is a light pseudoscalar particle introduced to solve the strong CP problem [1,2] and one of the most likely candidates for the dark matter. Therefore the axion is an extremely important particle for particle physics and astronomy.

In the interior of the Sun, blackbody photons can convert into axions in the fluctuating Coulomb fields of the charged particles in the plasma, $\gamma + (e^-, Ze) \rightarrow (e^-, Ze) + a$, and this reaction is called as the Primakoff process. Large number of current and proposed experiments are trying to detect thus-created solar axions [3–6].

The axion interacts so weakly with other particles that it escapes freely from the Sun once it is produced. Therefore it functions as an energy-loss mechanism. Schlattl et al. [7] calculated evolutionary solar models taking account of this axionic energy-loss. Comparing those models with constraints from helioseismology and neutrino oscillations, they derived a solar limit on the axion coupling to two photons $g_{a\gamma\gamma} < 10.0 \times 10^{-10} \text{ GeV}^{-1}$.

There are, however, some complaints about their approach as follows:

- Evolutionary solar models are constructed in the framework of stellar evolution, in which various assumptions about the past history of the Sun have to be adopted.
- Constraints from helioseismology are not effectively utilized.

Therefore we reexamine the calculation by using seismic solar models, which are free from evolutionary assumptions and utilize helioseismic constraints to

the full.

2 Seismic solar model

Helioseismology has been successful in determining precisely the sound-speed profile, $c(r)$, and the density profile, $\rho(r)$, in the Sun and the depth of the convection zone, r_{conv} , based on precise observations. By imposing the constraints of $c_{\text{obs}}(r)$, $\rho_{\text{obs}}(r)$, and r_{conv} , we can solve the basic equations governing the radiative core of the Sun (the continuity equation, the hydrostatic equation, the energy equation, and the energy transfer equation) directly without following the evolutionary history of the Sun. We call this model as the seismic solar model (hereafter SeiSM) and SeiSM is described in detail in Ref. [8]. SeiSM has advantages over the conventional solar models, evolutionary models, as follows:

- We can construct a model of the present-day Sun and evaluate the theoretically expected neutrino fluxes without assuming and following the evolutionary history of the Sun, which cannot be justified directly by observations.
- We can construct a model without worrying about the treatment of convection [9], which are not well-described theoretically.
- SeiSM is faithfully consistent with almost all observations ($c_{\text{obs}}(r)$, $\rho_{\text{obs}}(r)$, r_{conv} , luminosity, and the mass ratio of heavy elements to hydrogen at the surface, which is determined spectroscopically) except for the neutrino fluxes, while evolutionary models are not necessarily so, as shown later in Fig. 1 and 2.

3 Seismic solar models with axionic energy-loss

The axionic energy-loss rate by the Primakoff effect can be written in the form

$$\varepsilon_{\text{axion}} = 0.892 \times 10^{-3} g_{10}^2 T_7^7 \rho_2^{-1} F(\kappa^2) \text{ erg g}^{-1} \text{ s}^{-1}, \quad (1)$$

$$F(\kappa^2) = \frac{\kappa^2}{2\pi^2} \int_0^\infty dx \frac{x}{e^x - 1} \times \left[(x^2 + \kappa^2) \ln \left(1 + \frac{x^2}{\kappa^2} \right) - x^2 \right], \quad (2)$$

$$\kappa^2 \simeq 8.28 \rho_2 T_7^{-3} (3 + X), \quad (3)$$

where $g_{10} \equiv g_{a\gamma\gamma}/10^{-10} \text{ GeV}^{-1}$, $T_7 \equiv T/10^7 \text{ K}$, $\rho_2 \equiv \rho/10^2 \text{ g cm}^{-3}$, and X is the mass fraction of hydrogen [7,10,11]. We calculate a series of SeiSMs with varying $g_{a\gamma\gamma}$, which determines the amount of axionic energy-loss. The model's properties are summarized in Table 1. We show the axion luminosity, L_a , the temperature, T , and the mass fraction of heavy elements, Z , at the core, the mass fraction of helium, Y , at the surface, and the theoretically expected ^8B -neutrino flux and neutrino capture rates for the chlorine and the gallium experiments. In this procedure, SeiSMs are constructed so as to be always consistent with $c_{\text{obs}}(r)$ and $\rho_{\text{obs}}(r)$ (Fig. 1 and 2). In addition, Y_{surf} of thus-constructed SeiSMs are always in satisfactory agreement with the values determined directly from helioseismic inversions as demonstrated in Ref. [8].

We do not try to explain how SeiSM with axionic energy-loss can be realized in the evolutionary process, and such an investigation is beyond our scope. Our purpose is to clarify what can be derived if we construct self-consistent solar models with axionic energy-loss, which are faithfully consistent with almost

all observations except for the neutrino fluxes and free of severe subjective restrictions on the evolutionary history. In our opinion, assumptions in the standard evolutionary solar models (e.g. initial uniform chemical composition, no mass loss, and no accretion) are subjective restriction, which cannot be justified directly by observations.

An increase in the axionic energy-loss must be compensated by an increase in the nuclear energy generation, which leads to an increase in the theoretically expected neutrino fluxes. An increase in nuclear energy generation is realized with increases in T and ρ near the center of the Sun. However, ρ of SeiSM is constrained by observations, so T should increase particularly. A higher T_{core} means a steeper temperature gradient, which is proportional to the opacity. A higher opacity is realized with a higher Z . All these trends can be seen in Table 1, Fig. 3, and later in Fig. 4. Although Z -profiles shown in Fig. 3 may appear rough, it is sufficient to calculate the Z -profile of SeiSM to the third decimal place for discussing most of the properties of SeiSM other than the Z -profile, itself [8].

The density constraint and a non-uniform Z -profile make T_{core} of SeiSM very sensitive to $g_{a\gamma\gamma}$. Because the nuclear reaction rates are mainly controlled by T_{core} , the theoretically expected neutrino fluxes of SeiSM are more sensitive to $g_{a\gamma\gamma}$ than those of evolutionary solar models with a uniform Z -profile [7]. We found that if we construct seismic solar models with a uniform Z -profile [14], which are not necessarily consistent with $\rho_{\text{obs}}(r)$, by imposing the constraints of $c_{\text{obs}}(r)$ and r_{conv} , responses of the theoretically expected neutrino fluxes of such models to $g_{a\gamma\gamma}$ are similar to those of evolutionary solar models with a uniform Z -profile [7].

4 Solar neutrinos

Recently the Sudbury Neutrino Observatory (SNO) has announced the first results on solar neutrinos [15]. SNO detected the ^8B -neutrino via the charged current (CC) reaction on deuterium and by the elastic scattering (ES) of electrons. The CC reaction is sensitive exclusively to ν_e , while the ES reaction, the same reaction as the Super-Kamiokande (SK), is sensitive to all active neutrino flavors (ν_e, ν_μ, ν_τ), but with weak sensitivity to ν_μ and ν_τ . If there are flavor transformations between active neutrino flavors (ν_e, ν_μ, ν_τ), comparison of the neutrino flux deduced from the ES reaction assuming no neutrino oscillations, $\phi^{\text{ES}}(\nu_x)$, to that measured by the CC reaction, $\phi^{\text{CC}}(\nu_e)$, can provide the flux of non-electron flavor active neutrinos, $\phi(\nu_\mu, \nu_\tau)$. By comparing $\phi^{\text{CC}}(\nu_e)$ to the Super-Kamiokande's precise value of $\phi^{\text{ES}}(\nu_x)$ [16], the total flux of the active ^8B -neutrino, $\phi(\nu_e, \nu_\mu, \nu_\tau)$, is determined to be $5.44 \pm 0.99 \times 10^6 \text{cm}^{-2} \text{s}^{-1}$ [15]. If there are also oscillations to sterile neutrinos, the total flux may be slightly larger.

The neutrino flux derived in this way is consistent with the theoretically expected neutrino flux of SeiSM with $g_{a\gamma\gamma} = 0$. The relation of the observationally determined and the theoretically expected neutrino fluxes are shown in Fig. 4. We estimate the uncertainty of the theoretically expected neutrino flux by the method used in Ref. [8]. An increase in $g_{a\gamma\gamma}$ leads to an increase in the theoretically expected neutrino flux of SeiSM as explained in the previous section. Because a higher $g_{a\gamma\gamma}$ than a critical value makes the model's neutrino flux too high to be consistent with that determined from SNO and SK, we can limit $g_{a\gamma\gamma}$. From the comparison of these neutrino fluxes, we set a limit $g_{a\gamma\gamma} < 4.0 \times 10^{-10} \text{GeV}^{-1}$.

5 Conclusion

We calculate a series of seismic solar models (SeiSM) with varying the axion couplings to two photons, $g_{a\gamma\gamma}$, which determines the amount of axionic energy-loss. An increase in axionic energy-loss leads to increases in the nuclear reaction rates and the expected neutrino fluxes. The theoretically expected ^8B -neutrino flux of SeiSM should be identical with the total flux of the active neutrino flux, $\phi(\nu_e, \mu, \tau)$, which is determined by comparing the measured neutrino flux of the Sudbury Neutrino Observatory and that of the Super-Kamiokande. From the comparison of these neutrino fluxes, we set a limit $g_{a\gamma\gamma} < 4.0 \times 10^{-10} \text{ GeV}^{-1}$. This limit based on a new procedure is about a factor of 3 improvement over the previous theoretical limit [7] and a more severe limit than the solar axion experiments [3,4]. Therefore this limit is the most stringent limit on solar axions.

Acknowledgements

This research was supported in part by a Grant-in-Aid for Scientific Research on Priority Areas by the Japanese Ministry of Education, Culture, Sports, Science and Technology (12047208).

References

- [1] R.D. Peccei, H.R. Quinn, Phys. Rev. Lett. 38 (1977) 1440; Phys. Rev. D 16 (1977) 1791.

- [2] S. Weinberg, Phys. Rev. Lett. 40 (1978) 223; F. Wilczek, Phys. Rev. Lett. 40 (1978) 279.
- [3] SOLAX Collaboration, F.T. Avignone III et al., Phys. Rev. Lett. 81 (1998) 5068.
- [4] S. Moriyama et al., Phys. Lett. B. 434 (1998) 147.
- [5] S. Cebrián et al., Astrop. Phys. 10 (1999) 397.
- [6] K. Zioutas et al., Nucl. Instr. and Meth. A 425 (1999) 480.
- [7] H. Schlattl, A. Weiss, G. Raffelt, Astrop. Phys. 10 (1999) 353.
- [8] S. Watanabe, H. Shibahashi, submitted to Publ. Astron. Soc. Japan
- [9] M. Takata, H. Shibahashi, Astrophys. J. 504 (1998) 1035.
- [10] G.G. Raffelt, Phys. Rev. D 33 (1986) 897.
- [11] G.G. Raffelt, Stars as Laboratories for Fundamental Physics, The University of Chicago Press, 1996.
- [12] S. Basu, Mon. Not. R. Astron. Soc. 298 (1998) 719.
- [13] J.N. Bahcall, M.H. Pinsonneault, S. Basu, Astrophys. J. 555 (2001) 990.
- [14] S. Watanabe, H. Shibahashi, Publ. Astron. Soc. Japan 53 (2001) 565.
- [15] SNO Collaboration, Q.R. Ahmad et al., Phys. Rev. Lett. 87 (2001) 071301.
- [16] Super-Kamiokande Collaboration, S. Fukuda et al., Phys. Rev. Lett. 86 (2001) 5651.

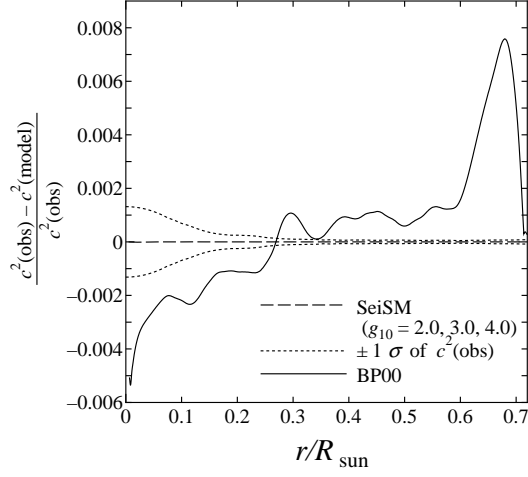


Fig. 1. Relative differences in the square of the sound-speed between seismic solar models with axionic energy-loss and the helioseismically determined profile [12], $c^2(\text{obs})$. For a comparison, the latest evolutionary model, BP00 [13], is also shown.

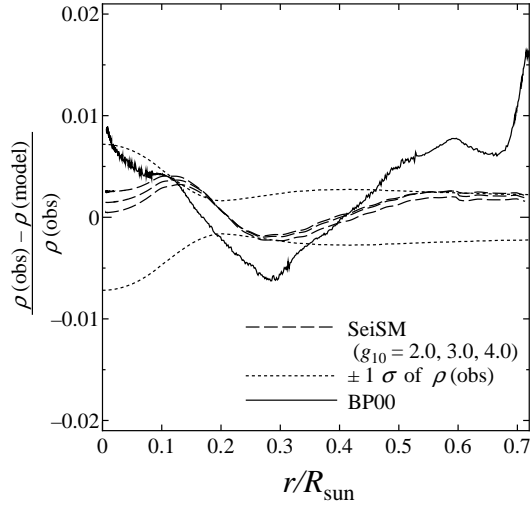


Fig. 2. Relative differences in the density. The line styles and references are the same as given in Fig. 1.

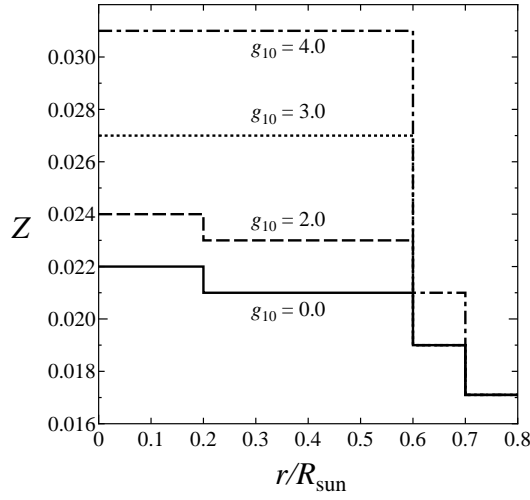


Fig. 3. Z -profiles of seismic solar models with different $g_{10} \equiv g_{a\gamma\gamma}/10^{-10} \text{ GeV}^{-1}$.

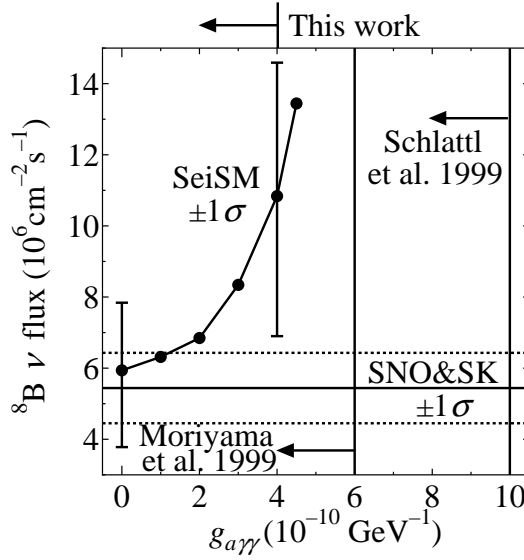


Fig. 4. The theoretically expected ${}^8\text{B}$ -neutrino fluxes of seismic solar models with different $g_{a\gamma\gamma}$. For a comparison, the observationally determined active neutrino flux is also shown by the horizontal solid line with the $\pm 1\sigma$ error band (the dotted lines). Vertical lines are upper limits for $g_{a\gamma\gamma}$: this work, the previous theoretical limit [7], and the most stringent limit from the solar axion experiments [4].

Table 1

Seismic solar models with axionic energy-loss

$g_{a\gamma\gamma}$ (10^{-10} GeV $^{-1}$)	0.0	3.0	4.0	4.5
L_a/L_\odot	0.000	0.019	0.037	0.050
T_{core} (10^7 K)	1.58	1.61	1.63	1.65
Z_{core}	0.022	0.027	0.031	0.035
Y_{surf}	0.240	0.240	0.240	0.240
Neutrino detection rates				
^8B (10^6 cm $^{-2}$ s $^{-1}$)	5.9	8.3	10.8	13.4
Cl (SNU*)	8.7	11.8	14.9	18.2
Ga (SNU)	132	147	161	175

* A SNU is defined to be 10^{-36} interactions s $^{-1}$ per target atom.